Efficient nonradiative energy transfer from InGaN/GaN nanopillars to CdSe/ZnS core/shell nanocrystals

Sedat Nizamoglu[1], Burak Guzelturk[1], Dae-Woo Jeon[2], In-Hwan Lee[2], and Hilmi Volkan Demir[1,3,*]

[1]Department of Electrical and Electronics Engineering, Department of Physics,

UNAM – National Nanotechnology Research Center, and Institute of Materials Science and Nanotechnology, Bilkent University, Ankara, Turkey TR-06800

[2]School of Advanced Materials Engineering, Research Center of Industrial Technology, Chonbuk National University, Chonju 561-756, Korea

[3] School of Electrical and Electronics Engineering and School of Physical and Mathematical Sciences, Nanyang Technological University, Nanyang Avenue, Singapore 639798, Singapore

*email: volkan@stanfordalumni.org

Supplementary Information

Additional information on multiple quantum well nanopillars: InGaN/GaN MQW epitaxial structure was grown by metal organic chemical vapor deposition (MOCVD). Trimethylgallium (TMGa), trimethylindium (TMIn) and NH_3 were used as precursors for Ga, In and N, respectively. A thermal annealing of c-plane sapphire substrate was performed at 1000°C for 10 min, followed by the growth of a low temperature GaN buffer layer. A 1 μm-thick undoped GaN layer and a 2 μm-thick n-type GaN layer were grown at 1060°C.

Subsequently, five pairs of InGaN/GaN MQW were grown on high quality GaN epitaxial layers and a 150 nm-thick p-GaN layer was directly grown on MQW layer.

A 100 nm-thick SiO_2 layer and 10 nm-thick Ni mask were deposited on the epi-wafer surface by plasma-enhanced CVD and e-beam evaporator, respectively. This epi-wafer was subsequently annealed under flowing N_2 at a temperature of 800°C for 1 min to form Ni clusters. Then, SiO_2 and GaN layers were etched for 120 s and 5 min using an ICP-RIE process, respectively. Finally, Ni metal and SiO_2 layers were removed by buffered oxide etchant (BOE). The nanopillar formation steps are schematically illustrated in Fig. S1(a). In Fig. S1(b) the scanning electron microscopy (SEM) image reveals that the nanopillars are finely formed. Furthermore, the existence of multiple quantum wells in both planar structure and nanopillars are shown by using x-ray diffraction (XRD) measurements depicted in Fig. S1(c).

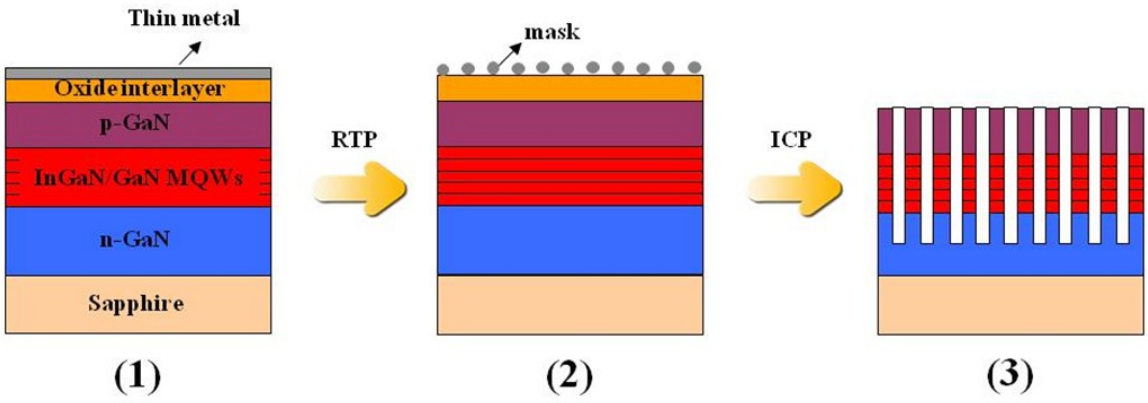

(a)

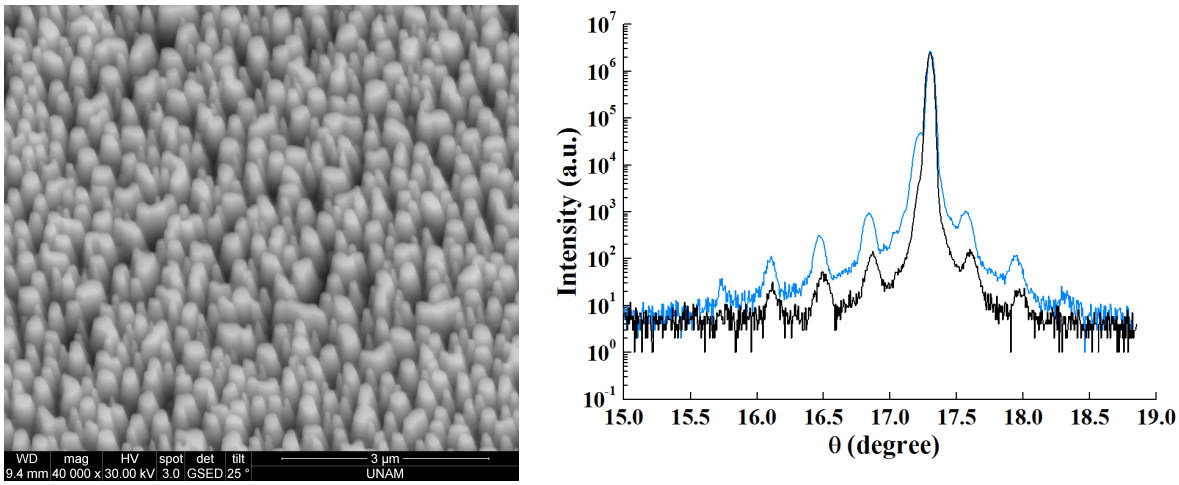

(b) **(c)**

Fig. S1. (a) Schematic representation of the nanopillar formation, (b) scanning electron microscopy image of the fabricated InGaN/GaN multiple quantum well nanopillars, and (c) x-ray diffraction measurement.

Additional information on nanocrystal quantum dots: Our green-, yellow- and red-emitting nanocrystal quantum dots (NQDs) have molecular weights of 94, 140, 270 µg/nmol and their corresponding diameters are ca. 3.3, 3.8 and 5.0 nm with a size dispersion of <5%, respectively. They have a concentration of 10 mg/mL and exhibit in-solution quantum efficiencies of >50%. In Fig. S2, absorption and emission spectra of CdSe/ZnS core/shell nanocrystal quantum dots are shown, along with photoluminescence spectra of both planar and nanopillar structures of InGaN/GaN multiple quantum wells.

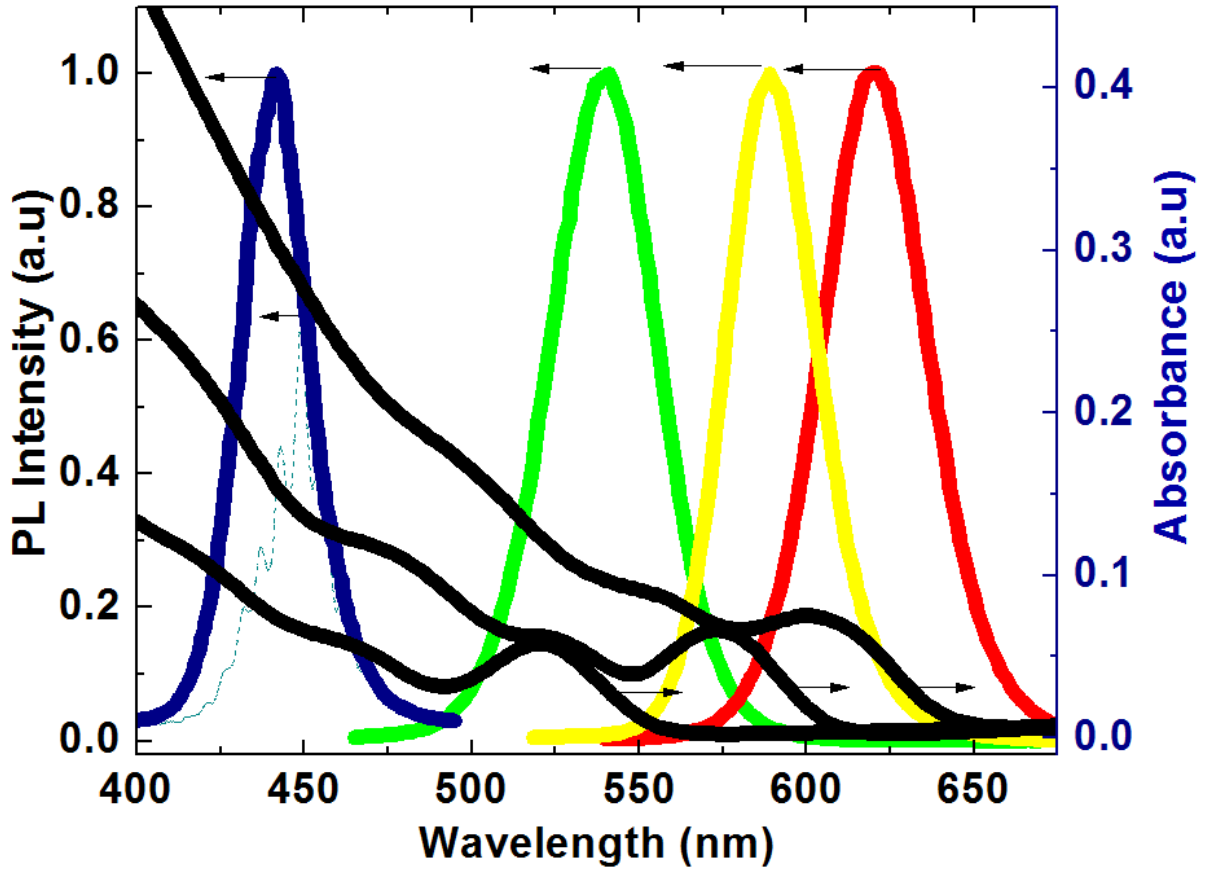

Fig. S2. Photoluminescence spectra of both blue-emitting planar (solid line) and nanopillar (dashed line) structures of InGaN/GaN multiple quantum wells, and absorption and emission spectra of green-, yellow- and red-emitting CdSe/ZnS core/shell nanocrystal quantum dots.

Additional information on time-correlated single photon counting (TCSPC) system of PicoHarp 300: PicoHarp 300 (from PicoQuant GmbH, Germany) provides a highly stable and crystal calibrated time resolution of 4 ps.[1] As the detector, the system includes a photon multiplier detector array (PMA), which is based on the Hamamatsu H5783 series photosensor module. PMA unit consists of built-in high voltage power supply, signal pre-amplifier and a gold plated iron, allowing for optimal timing performance. For the pump, the system houses a

LDH-D-C-375 laser head controlled by a PDL-800B driver, which provides picosecond laser pulses at 375 nm.

Additional information on lifetime analyses: For the lifetime analysis of only nanopillar case given in Fig. S1, we use Eq. S1, where IRF(t) is the instrument response function, A is the amplitude, and τ_{np} is the lifetime of the nanopillars.

$$I_{fit}(t) = \int_{-\infty}^{t} IRF(t')\left(Ae^{-\frac{(t-t')}{\tau_{np}}}\right)dt' \qquad \text{(S1)}$$

For the case of MQW-NPs hybridized with NQDs presented in Fig. 1, (and also for those depicted in Figs. S3 and S4 in the supplementary material[16]), we use Eq. S2, where τ_{ET} is the nonradiative energy transfer lifetime, because the generated electron-hole pairs near to NQDs (with a distance comparable to or less than 2×Förster radius) make nonradiative energy transfer, but those farther away from the NQDs do not.

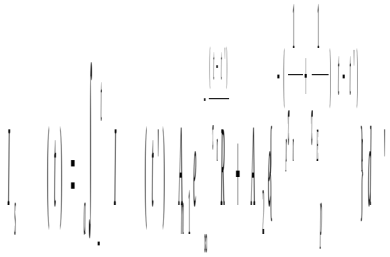

(S2)

The spectral overlap is calculated by using Eq. S3, where $F_D(\lambda)$ is the corrected fluorescence intensity of the donor and $\varepsilon_A(\lambda)$ is the extinction coefficient of the acceptor at the wavelength of λ.[2]

$$J(\lambda) = \int_0^{\infty} F_D(\lambda)\varepsilon_A(\lambda)\lambda^4 d\lambda \qquad \text{(S3)}$$

The energy transfer efficiency is calculated by using Eq. S4, where k_{ET} is the nonradiative energy transfer rate and k_{NP} is the nanopillar recombination lifetime.

$$\eta_{ET} = \frac{k_{ET}}{(k_{ET} + k_{NP})} \qquad \text{(S4)}$$

Time-resolved measurements of multiple quantum well nanopillars integrated with yellow- and green-emitting nanocrystal quantum dots: The time-resolved and steady-state spectroscopy data of the hybrid case of the nanopillars hybridized with yellow-emitting NQDs are shown in Fig. S3; and those, for green-emitting NQDs, in Fig. S4.

.

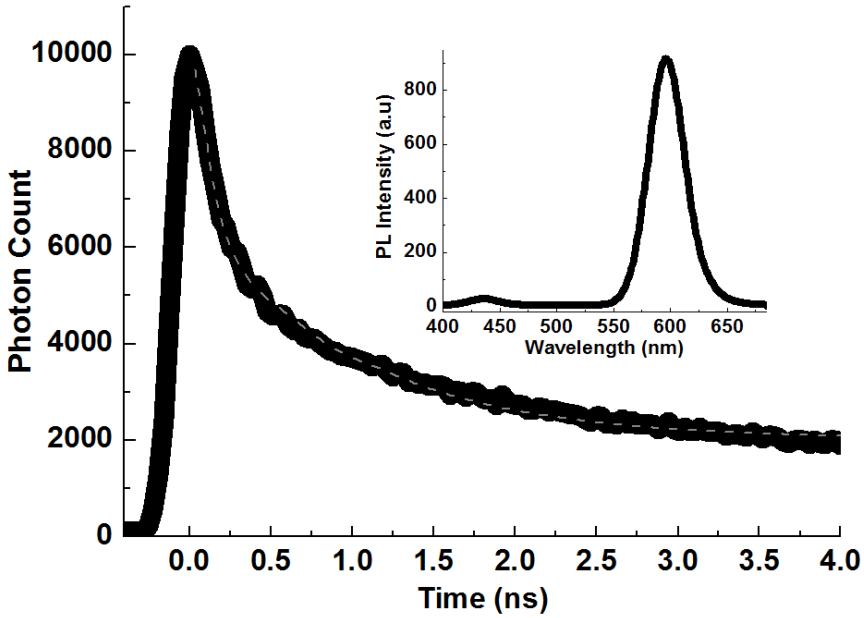

Fig. S3. MQW-NPs photoluminescence decay (at λ= 450 nm) with yellow-emitting NQDs. The dashed lines are the numerical fits as described in text. Inset exhibits steady-state photoluminescence spectrum of MQW-NPs with these yellow-emitting NQDs.

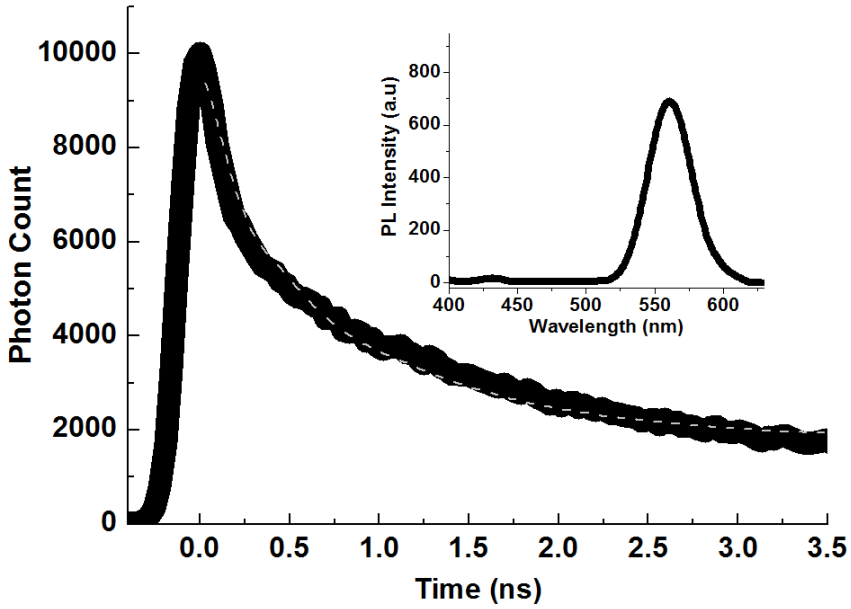

Fig. S4. MQW-NPs photoluminescence decay (at λ= 450 nm) with green-emitting NQDs. The dashed lines are the numerical fits as described in text. Inset exhibits steady-state photoluminescence spectrum of MQW-NPs with these green-emitting NQDs.

Derivation of the energy transfer rate from multiple quantum well to nanocrystal quantum dots: We perform computational analysis of electron-hole pair transfer rates to further understand the energy transfer process by deriving the exciton transfer formula for our hybrid architectures. According to our model, MQWs transfer their excitons to NQD layer at the surface of the nanopillars. We calculate the expected ET rates by following Eqs. S5-S7.

$$R_{ET}(r) = \frac{1}{\tau_{MQW}} \left(\frac{R_0}{r}\right)^4 \qquad \text{(S5)}^2$$

$$C = k_D R_0^6 \qquad \text{(S6)}^3$$

$$
\begin{aligned}
k_{ET} &= CR^{-6} \\
&= \sigma R_0{}^6 \int_0^\infty k_{ET}\, dS \\
&= k_D \sigma R_0{}^6 \int_0^\infty \frac{2\pi\rho}{(d^2+\rho^2)^3} d\rho \\
&= k_D \sigma R_0{}^6 2\pi(-1)\left[\frac{1}{4(d^2+\rho^2)^2}\right]_0^\infty \\
&= \frac{k_D 0.5\pi\sigma R_0{}^6}{d^4}
\end{aligned}
\tag{S7}
$$

Table SI lists parameters used to calculate ET rate for different samples of MQW-NPs with red-, green- and yellow-emitting NQDs.

Table SI. Parameter values used to calculate ET rate for different samples. MQW-NPs with red-, green- and yellow-emitting NQDs are dubbed Sample # 1, 2 and 3, respectively. k_{ET} is the calculated ET rate, R_o is the Förster radius, J is the spectral overlap between the emission of the nanopillars and absorption of NQDs, n is the effective refractive index of the interaction medium, d is the interspacing between the center of the NQDs and NPs, and σ is the dot density given in terms of number of NQDs per cm^2.

Sample #	k_{ET} (ns^{-1})	R_0 (nm)	J ($M^{-1}cm^1nm^4$)	n	d (nm)	σ (cm^{-2})
1	$(0.197)^{-1}$	5.777	4.421×10^{16}	1.934	4	2.100×10^{12}
2	$(0.230)^{-1}$	4.887	1.491×10^{16}	1.894	3.5	2.872×10^{12}
3	$(0.248)^{-1}$	4.164	4.933×10^{15}	1.874	3	4.164×10^{12}

References

[1] http://www.picoquant.com/ (accessed Aug 30, 2010).

[2] J. R. Lakowicz, Principles of Fluorescence Spectroscopy (Springer, New York, 2006).

[3] D. Kim, S. Okahara, M. Nakayama and Y. Shim, Phys. Rev. B **78**, 153301 (2008).